
Progressive Neural Architecture Search

Chenxi Liu^{*1} Barret Zoph² Jonathon Shlens² Wei Hua³ Li-Jia Li³ Li Fei-Fei^{3,4} Alan Yuille¹
Jonathan Huang⁵ Kevin Murphy⁵

Abstract

We propose a method for learning CNN structures that is more efficient than previous approaches: instead of using reinforcement learning (RL) or genetic algorithms (GA), we use a sequential model-based optimization (SMBO) strategy, in which we search for architectures in order of increasing complexity, while simultaneously learning a surrogate function to guide the search, similar to A* search. On the CIFAR-10 dataset, our method finds a CNN structure with the same classification accuracy (3.41% error rate) as the RL method of Zoph et al. (2017), but 2 times faster (in terms of number of models evaluated). It also outperforms the GA method of Liu et al. (2017), which finds a model with worse performance (3.63% error rate), and takes 5 times longer. Finally we show that the model we learned on CIFAR also works well at the task of ImageNet classification. In particular, we match the state-of-the-art performance of 82.9% top-1 and 96.1% top-5 accuracy.

1. Introduction

Deep neural networks have demonstrated excellent predictive performance on many tasks. In particular, ever since the seminal work of Krizhevsky et al. (2012), image classification has been dominated by convolutional neural networks (CNNs) of various architectures (see e.g., (Simonyan & Zisserman, 2015; Szegedy et al., 2015; 2016; He et al., 2016; Huang et al., 2017b)). All of these widely-used neural network architectures are designed by people, but this process is laborious and requires experience and expertise. Hence there has been a lot of recent interest in automatically learning good neural net architectures.

Current techniques usually fall in one of two categories: genetic algorithms (see e.g. (Real et al., 2017; Miikkulainen

et al., 2017; Xie & Yuille, 2017)) or reinforcement learning (see e.g., (Zoph & Le, 2017; Zoph et al., 2017; Zhong et al., 2018; Cai et al., 2017; Baker et al., 2017a)). In genetic algorithms (GA), each neural network specification is encoded as a string, and random mutations and recombinations of the strings are performed during the search process; each string (model) is then trained and evaluated on a validation set, and the top performing models generate “children”. Under the reinforcement learning (RL) formulation, the system performs a sequence of actions, which specifies the structure of the model; this model is then trained and its validation performance is returned as the reward function, which is used to update the RNN controller. Although such methods have been able to learn network structures that outperform manually designed architectures, they require significant computational resources. For example, the RL method in Zoph et al. (2017) trains and evaluates 20,000 neural networks across 500 P100 GPUs over 4 days.

In this paper, we describe a method that is able to learn a CNN which matches previous state of the art while requiring roughly half as many model samples during the architecture search. Our starting point is the structured search space proposed by Zoph et al. (2017), in which the search algorithm is tasked with searching for a good convolutional “cell”, as opposed to a full CNN. A cell contains B “blocks”, where a block is a combination operator (such as addition) applied to two inputs (tensors), each of which can be transformed (e.g., using convolution) before being combined. This cell structure is then stacked a certain number of times, depending on the size of the training set, and the desired running time of the final model. Although the structured space simplifies the search process significantly, the number of possible cell structures is still exponentially large. Thus, many opportunities exist for searching this space more efficiently.

Our approach is similar to the A* algorithm (also called branch and bound), in that we search the space of models from simple to complex, pruning out unpromising models as we go. The models (cells) are ordered by the number of blocks they contain. We start by considering cells with one block. We evaluate these cells (by training them and then computing their loss on a validation set), and use the observed reward to train an heuristic function (also called

^{*}Work done while an intern at Google ¹Johns Hopkins University ²Google Brain ³Google Cloud ⁴Stanford University ⁵Google AI. Correspondence to: Chenxi Liu <cqliu@jhu.edu>.

a surrogate function) based on an RNN, which can predict the reward for any model. Using this learned heuristic function, we decide which cells with 2 blocks we should evaluate. After evaluating them, we update the heuristic function. We repeat this process until we find good cells with the desired number of blocks.

Our progressive (simple to complex) approach has several advantages. First, the simple models train faster, so we get some initial results to train the surrogate quickly. Second, we only ask the surrogate to predict the quality of models that are slightly different from the ones it has seen (c.f., trust-region methods). Third, we factorize the search space into a product of smaller search spaces.

In summary, we present an approach for CNN structure learning that is roughly two times more efficient than the best previous method while achieving the same quality results. We believe that our approach will allow us to scale up architecture search to more complex search spaces, and larger datasets.

2. Related Work

Zoph & Le (2017) propose a method based on RL called “neural architecture search” (NAS). In particular, they use the REINFORCE algorithm (Williams, 1992) to estimate the parameters of a recurrent neural network (RNN); the RNN represents a policy which generates a sequence of symbols (actions) specifying the structure of the CNN; the reward function is the classification accuracy on the validation set of a CNN generated from this sequence. We will call this the NAS-RL method.

Zoph et al. (2017) extend their prior work in two ways. First, they replace REINFORCE with proximal policy optimization (PPO) (Schulman et al., 2017). Second, they use a more carefully designed search space consisting of stacked CNN cells, rather than completely unstructured CNNs. We will call this method NAS-RL-cell, to distinguish it from the original NAS-RL method. The NAS-RL-cell method was able to learn CNNs which outperformed almost all previous methods in terms of accuracy vs speed on image classification (CIFAR-10 (Krizhevsky & Hinton, 2009) and ImageNet (Deng et al., 2009)) and object detection (MS COCO (Lin et al., 2014)) datasets.

There are several other papers that use RL to learn network topologies. Zhong et al. (2018) use the same model search space as NAS-RL-cell, but replace policy gradient with Q-learning. Baker et al. (2017a) also use Q-learning, but without exploiting cell structure. Cai et al. (2017) use policy gradient to train an RNN, but the actions are now to widen an existing layer, or to deepen the network by adding an extra layer. This requires specifying an initial model and then gradually learning how to transform it.

An alternative to RL is to use genetic algorithms (GA) to search through the space of neural networks models (this is known as “neuro-evolution” (Stanley, 2017)). Early work (e.g., (Stanley & Miikkulainen, 2002)) used GA to learn both the structure and the parameters of the network, but more recent methods, such as (Real et al., 2017; Miikkulainen et al., 2017; Xie & Yuille, 2017; Liu et al., 2017), just use GA to search the structures, and use SGD to estimate the parameters.

Negrinho & Gordon (2017) use Monte Carlo Tree Search (MCTS) to search through the space of CNN architectures. MCTS searches the space of models in a shallow-to-deep way, but at each node in the search tree, it uses random selection to choose which branch to expand, which is very inefficient.

Sequential Model Based Optimization (SMBO) (Hutter et al., 2011) improves on MCTS by learning a predictive model, which can be used to decide which nodes to expand. This technique is used in several other papers (e.g., (Mendoza et al., 2016; Negrinho & Gordon, 2017)), but none have shown the kinds of gains on large scale image classification problems that we do.

Several papers learn a surrogate function to predict model performance without training it (e.g., (Baker et al., 2017b; Negrinho & Gordon, 2017; Mendoza et al., 2016)), but these methods were applied to fixed sized models, and would not work with our progressive search approach. Furthermore, their learned models do not come close to our state of the art results.

Brock et al. (2017) train one network to predict the weights of another network, thereby significantly speeding up the evaluation of a candidate model. They then evaluate this model using the predicted weights, and call the resulting quality estimate the “SMASH score” of a model. They use this technique, combined with random search, to find good models. However, the models we learn are substantially better than the ones they discover. We believe there are several reasons for this. First, predicting the quality of a model (from a string specification) is a much easier task than predicting all its parameters; second, searching the space progressively is much more efficient than random search; and third, searching the space of cells is much more efficient than searching the space of full CNNs.

Several groups have performed architecture search by incrementally increasing the complexity of the model: Stanley & Miikkulainen (2002) used a similar approach in the context of evolutionary algorithms, Zoph & Le (2017) used a schedule of increasing number of layers, and Grosse et al. (2012) used a similar approach to systematically search through the space of latent factor models specified by a grammar. Finally, Cortes et al. (2017); Huang et al. (2017a)

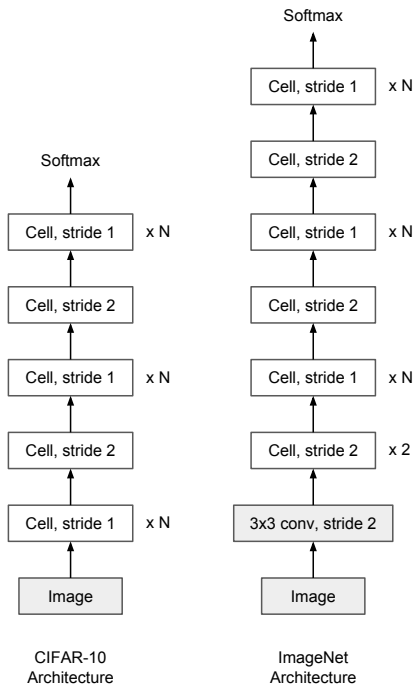


Figure 1. Network architecture for CIFAR-10 and ImageNet from Zoph et al. (2017). Note that we learn a single cell type instead of distinguishing between Normal and Reduction cell.

grow CNNs sequentially using boosting; however, their results do not improve the accuracy over manual designs.

3. Architecture Search Space

In this section we describe the neural network architecture search space used in our work. We employ a reduced version of the search space in Zoph et al. (2017).

Figure 1 provides a diagram of the network architecture employed in our experiments parallel to Zoph et al. (2017). Given a convolutional cell topology (labeled *Cell*), we repeat the cell a variable number of times so we may control the resulting model complexity. Specifically, we insert more stride 2 cells in the stacked architecture for the network that is trained on ImageNet since the spatial scale of the images (e.g. 224×224 or 331×331) is much larger than CIFAR-10. We employ a common heuristic to double the number of filter channels whenever the spatial activation map is reduced by a stride of 2. The final output of the network is obtained by applying global average pooling on the last feature map, followed by a softmax transformation. Thus a network structure is fully specified by defining the cell topology, the initial filter count F and the number of cell repetitions N . The remainder of this section is devoted to a discussion of the construction of the convolutional cell.

The goal of the architecture search procedure is to find the best transferable and reusable cell topology. The cell is parameterized as a DAG consisting of B blocks. Each block is a mapping from 2 input tensors to 1 output tensor. We can specify a block b in a cell c as a 5-tuple, (I_1, I_2, O_1, O_2, C) , where $I_1, I_2 \in \mathcal{I}_b$ specifies the inputs to the block, $O_i \in \mathcal{O}$ specifies the operation to apply to input I_i , and $C \in \mathcal{C}$ specifies how to combine O_1 and O_2 to generate the feature map (tensor) corresponding to the output of this block, which we denote by H_b^c .

The set of possible inputs, \mathcal{I}_b , is the set of all previous blocks in this cell, $\{H_1^c, \dots, H_{b-1}^c\}$, plus the final block in the previous cell, H_B^{c-1} , plus the final block in the previous-previous cell, H_B^{c-2} .

The operator space \mathcal{O} is the following set of 8 functions, each of which operates on a single tensor:

- 3x3 depthwise-separable convolution
- 5x5 depthwise-separable convolution
- 7x7 depthwise-separable convolution
- identity
- 3x3 average pooling
- 3x3 max pooling
- 3x3 dilated convolution
- 1x7 followed by 7x1 convolution

This is less than the 13 operators used in Zoph et al. (2017), since we removed the ones that their RL method discovered were never used.

Finally, we fix the combination operator C to be the element-wise addition of two tensors. This is less than the 2 combination operators used in Zoph et al. (2017), since we removed the one (namely concatenation) that their RL method discovered was never used.

We now quantify the size of the search space to highlight the magnitude of the search problem. Let the space of possible structures for the b 'th block be \mathcal{B}_b , which has size $|\mathcal{B}_b| = |\mathcal{I}_b|^2 \times |\mathcal{O}|^2 \times |\mathcal{C}|$, where $|\mathcal{I}_b| = (2+b-1)$, $|\mathcal{O}| = 8$ and $|\mathcal{C}| = 1$. For $b = 1$, we have $\mathcal{I}_1 = \{H_B^{c-1}, H_B^{c-2}\}$, which are the final outputs of the previous two cells, so there are $|\mathcal{B}_1| = 256$ possible block structures. If we allow cells of up to $B = 5$ blocks, the total number of cell structures is given by $|\mathcal{B}_{1:5}| = 2^2 \times 8^2 \times 3^2 \times 8^2 \times 4^2 \times 8^2 \times 5^2 \times 8^2 \times 6^2 \times 8^2 = 5.6 \times 10^{14}$.

Note that this is smaller than the search space used in Zoph et al. (2017), which has size 10^{28} , since they learn both Normal and Reduction cells, whereas we just learn Normal cells. (We also use 8 unary operators instead of 13, and 1 binary operator instead of 2.) Nevertheless, it is still an extremely large space to search.

4. Method

4.1. Progressive Neural Architecture Search

To construct a cell, we need to combine B blocks. Unfortunately, the size of the search space grows exponentially with B . As shown above, even if we just use $B = 5$, there are $|\mathcal{B}_{1:5}| \sim 10^{14}$ possible cell structures.

Many previous approaches directly work with this final, large search space. For example, NAS-RL-cell uses a 50-step RNN¹ as a controller to generate model specifications. In Xie & Yuille (2017) a fixed-length binary string encoding of CNN architecture is defined and used in model evolution/mutation. While this is a more direct approach, we argue that it is difficult to directly navigate in an exponentially large search space, especially at the beginning where there is no knowledge of what makes a good model.

As an alternative, we propose to search the space in a progressive order, simplest models first. In particular, we start by constructing all possible cell structures from \mathcal{B}_1 (i.e., composed of 1 block), and add them to a queue. We train and evaluate all the models in the queue (in parallel), and then expand each one by adding all of the possible block structures from \mathcal{B}_2 ; this gives us a set of $|\mathcal{B}_1| \times |\mathcal{B}_2| = 256 \times 576 = 147,456$ candidate cells of depth 2. Since we cannot afford to train and evaluate all of these child networks, we apply a learned predictor function (described in Section 4.2) to predict their score; this is trained based on the measured performance of the cells we have visited so far. (Our predictor takes negligible time to train and apply.) We then use the predictor to evaluate all the candidate cells (which could be done in parallel), and pick the K most promising ones. We add these to the queue, and repeat the process, until we find cells with a sufficient number B of blocks. See Algorithm 1 for the pseudocode, and Figure 2 for an illustration.

Note that we currently greedily pick the top K models at each iteration. We could instead follow the technique used in the Bayesian optimization (BO) literature (see e.g., (Snoek et al., 2012; Shahriari et al., 2016)) in which we use an acquisition function, such as expected improvement or upper confidence bound, to rank the candidate models; this takes into account uncertainty in the prediction of a model’s performance, which encourages us to try models for which our predictor may be unreliable. This requires that our predictor be able to compute $\mu(m) = E[r|m, \mathcal{D}]$, the mean of the posterior predictive distribution over the reward (validation loss) of model m given the data \mathcal{D} seen so far, and $\sigma(m) = \sqrt{\text{Var}[r|m, \mathcal{D}]}$, the standard deviation of this posterior. However, we leave the integration of BO methods with PNAS to future work.

¹ They need to generate 5 symbols per block, times 5 blocks, times 2, for Normal and Reduction cells.

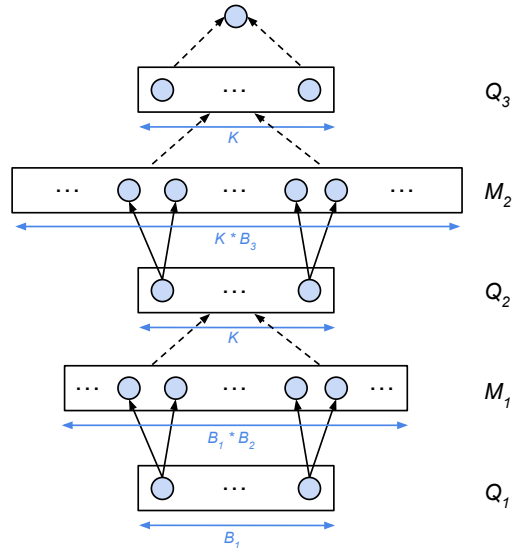


Figure 2. Illustration of the PNAS search procedure when the maximum number of blocks is $B = 3$. Here \mathcal{Q}_b represents the set of candidate cells with b blocks. We start by consider all cells with 1 block, $\mathcal{Q}_1 = \mathcal{B}_1$; we train and evaluate all of these cells, and update the predictor. At iteration 2, we expand each of the cells in \mathcal{Q}_1 to get all cells with 2 blocks, $\mathcal{M}_2 = \mathcal{B}_{1:2}$; we predict their scores, pick the top K to get \mathcal{Q}_2 , train and evaluate them, and update the predictor. At iteration 3, we expand each of the cells in \mathcal{Q}_2 , to get a subset of cells with 3 blocks, $\mathcal{M}_3 \subseteq \mathcal{B}_{1:3}$; we predict their scores, pick the top K to get \mathcal{Q}_3 , train and evaluate them, and return the winner. Blue horizontal lines denote the sizes of each set, where $B_b = |\mathcal{B}_b|$ is the number of possible blocks at level b and K is the beam size.

4.2. Accuracy Prediction with Encoder RNN

As explained above, we need a mechanism to predict the final classification accuracy of a cell given its specification; this is known as a surrogate function. There are at least three desired properties of such a predictor:

- *Close to true value:* The more accurate the prediction, the more we can rely on it to efficiently prune out unpromising model specifications.
- *Handle variable-sized models:* We need the predictor to work for variable-length input strings. In particular, it should be able to predict the performance of any cell with $b + 1$ blocks, even if it has only been trained on a subset of cells with up to b blocks.
- *Sample efficiency:* We hope to train and evaluate as few child networks as possible, which means the training data for the accuracy predictor will be scarce.

Consequently, we choose to use a recurrent neural network (RNN) as our predictor, since RNNs are known to be ac-

Algorithm 1 Progressive Neural Architecture Search (PNAS).

Input:
 F // # of filters in first layer
 N // # of times to unroll the cells
 B // Max. # of blocks in a cell
 K // Max. # of models to evaluate per iter.
trainSet // training set
valSet // validation set
begin
 $\mathcal{Q}_1 = \mathcal{B}_1$ // Set of models with one block
pred = init-predictor() // Surrogate predictor (RNN)
for $b = 1 : B - 1$ **do**
 // Train and evaluate current set of models in \mathcal{Q}
 $\mathcal{D}_b = []$ // Store evaluated models and scores
 for $m \in \mathcal{Q}_b$ **do**
 model = train(unroll(m, F, N), trainSet)
 score = eval(models[m], valSet)
 \mathcal{D}_b .push(model, score)
 end for
 // Update predictor based on new data
 pred = pred.update(\mathcal{D}_b)
 // Expand and predict the search beam
 $\mathcal{M}_{b+1} = []$ // Store future candidate models
 $\mathcal{S}_{b+1} = []$ // Store predicted scores
 for $m \in \mathcal{Q}_b$ **do**
 $\mathcal{C} = \text{expand-by-one-block}(m)$ // Children
 for $c \in \mathcal{C}$ **do**
 \mathcal{M}_{b+1} .push(c)
 \mathcal{S}_{b+1} .push(pred.predict(c))
 end for
 end for
 // Pick the most promising candidates
 $\mathcal{Q}_{b+1} = \text{top-K}(\mathcal{M}_{b+1}, \mathcal{S}_{b+1}, K)$
end for
Return top-K($\mathcal{M}_B, \mathcal{S}_B, 1$)
end

curate and can easily handle variable-sized inputs; furthermore, our supervised learning approach is much more sample efficient than RL methods.

In more detail, each block of the input cell is specified by 4 symbols, corresponding to $\mathcal{I}_1, \mathcal{I}_2, \mathcal{O}_1$ and \mathcal{O}_2 (recall that we assume \mathcal{C} is fixed to a single combination operator). We unroll this for B steps, but the embeddings of \mathcal{I} and \mathcal{O} are shared across blocks. We use an LSTM whose final hidden state is followed by a fully connected layer and sigmoid nonlinearity to regress to the validation accuracy (a scalar in range $[0, 1]$).

At iteration b of the PNAS algorithm, we update the parameters of the predictor using the data collected during this iteration, $\mathcal{D}_b = \{(x, y)\}$, where x is one of the top K

models, and y is the validation loss of that model, using a few steps of SGD.

Note that the encoder RNN used here is very different from the decoder RNN used in NAS-RL: we use the RNN to predict the score of a candidate model generated by a search process, whereas they use the RNN to generate candidate models.

5. Experiments and Results

5.1. Experimental Details

Our experimental setting follows Zoph et al. (2017). In particular, we conduct most of our experiments on CIFAR-10 (Krizhevsky & Hinton, 2009), and then see how well the resulting model works on ImageNet (Deng et al., 2009) classification.

CIFAR-10 has 50,000 training images and 10,000 test images. We use 5000 images from the training set as a validation set. All images are whitened, and 32x32 patches are cropped from images upsampled to 40x40. Random horizontal flip is also used.

For the accuracy predictor, the LSTM hidden state size and embedding size are both 100. The bias term in the final fully connected layer is initialized to 1.8 (0.86 after sigmoid) to account for the mean observed accuracy of all $b = 1$ models. The embeddings use uniform initializer in range $[-0.1, 0.1]$. We use the Adam optimizer (Kingma & Ba, 2015) with learning rate 0.01 for the $b = 1$ level and 0.002 for all following levels. We use L_1 loss to train the surrogate predictor.

Our training procedure for the CNNs follows the one used in Zoph et al. (2017). During the search we evaluate $K = 256$ networks at each stage, we use a maximum cell depth of $B = 5$ blocks, we use $F = 24$ filters in the first convolutional cell, we unroll the cells for $N = 2$ times, and each child network is trained for 20 epochs using initial learning rate of 0.01 with cosine decay (Loshchilov & Hutter, 2017). After finding the best model, we increase N and F , and train it for 600 epochs using initial learning rate of 0.025 with cosine decay. During training we also used auxiliary classifier located at 2/3 of the maximum depth weighted by 0.4, and drop each path with probability 0.4 for regularization.

5.2. Efficiency of PNAS

We now discuss the efficiency of the algorithm. At iteration b , we have K cells in the queue; each cell generates $|\mathcal{B}_{b+1}|$ children, which get added to a list; we predict their scores, pick the top K , and then train and evaluate these “survivors”. Thus the total number of models that we train and evaluate is $|\mathcal{B}_1| + K \times (B - 1)$. In our experiments,

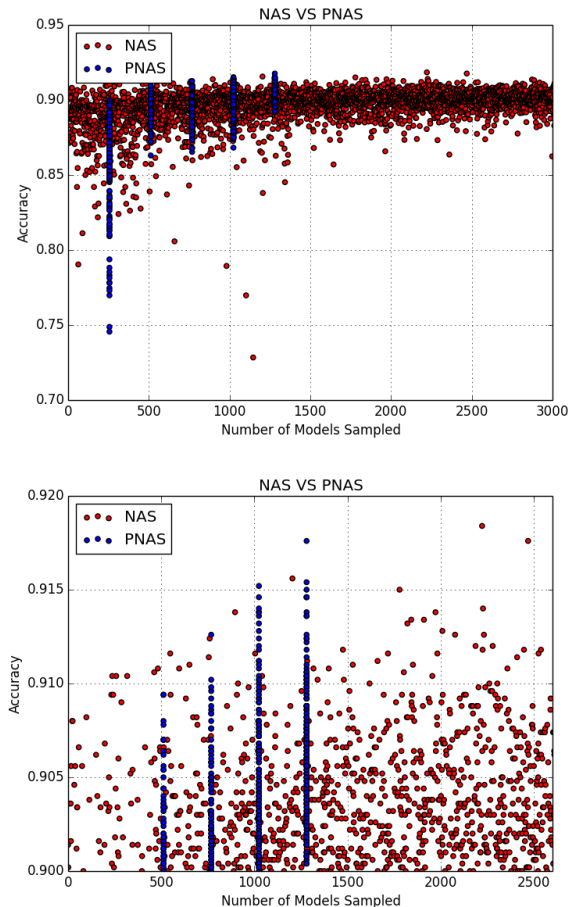


Figure 3. Comparing the relative efficiency of NAS and PNAS algorithms. Validation accuracy on CIFAR-10 validation set of the first 1280 models visited by PNAS (blue) and the first 3000 models visited by NAS-RL (red). Bottom is zoomed in section of the top graph. The PNAS results come in $B = 5$ clusters, reflecting the B stages of the algorithm. After 1280 models PNAS achieves top-1 accuracy of 0.917, a mean top-5 accuracy of 0.915 and a mean top-25 accuracy of 0.912. After 2280 models, NAS-RL achieves a top-1 accuracy of 0.917, a mean top-5 accuracy of 0.915 and a mean top-25 accuracy of 0.913. Note that the *mean* top accuracies smooth over some of the stochastic fluctuations of the architecture search algorithms.

$|\mathcal{B}_1| = K = 256$ and $B = 5$, so we train and evaluate 1280 models.

In Figure 3 we compare the PNAS method to the NAS-RL-cell method. Both methods were run on the same search space, namely the one with size 10^{14} . We see that the accuracy (on the validation set) of the PNAS models increases as b increases, as is to be expected. At the end of its search through 1280 models, the method reaches a peak accuracy of 0.917, a mean top-5 accuracy of 0.915 and a mean top-25 accuracy of 0.912. Note that there is a degree of stochas-

ticity in these numbers due to random initialization of the model weights and the stochasticity of random data augmentations and SGD batching.

By contrast, the RL method matches the top-1 accuracy of 0.917 after 2280 models have been sampled. The RL algorithm exhibits the same stochastic variability as PNAS due to the variability of training a CIFAR-10 model. In addition, the RL algorithm exhibits additional significant stochasticity due to the sampling of the RNN outputs. This sampling permits a greater diversity of model exploration as seen in the greater variance of the red dots.

Given the amount of stochasticity in the RL algorithm, we focus on a comparison of the mean top-5 and mean top-25 performances of all of the models sampled. After 2280 models, RL achieves a mean top-5 accuracy of 0.915 and a mean top-25 accuracy of 0.913. These numbers are roughly comparable to PNAS and support the contention that PNAS requires roughly $1.8\times$ fewer models to achieve similar performances. Additional experiments, however, are required to understand the relative efficiency of this algorithm in larger search spaces.

Note that each dot in Figure 3 corresponds to training a model from scratch for 20 epochs on CIFAR. (The blue PNAS dots for $b < 5$ are slightly cheaper to train than the red NAS dots, since they are smaller models.) We could easily use methods, such as those in Baker et al. (2017b), which apply early stopping to “unpromising” models. This would reduce the amount of time it takes to evaluate each of the dots. We could also consider methods that select fewer than K models at each iteration of PNAS. However, we leave these extensions to future work.

5.3. Results on CIFAR-10 Image Classification

We now discuss the performance of our final model when trained for 600 epochs (as opposed to the 20 epochs used during search), and compare it to the results of other methods in the literature. The results are shown in Table 1.

We see that our best model PNASNet-5 achieves the same error rate (3.41%) as the NASNet-A model from Zoph et al. (2017). However, we only need to evaluate 1280 models in total to find this model, which is $15\times$ fewer models than the 20,000 models evaluated by the NAS-RL-cell method. Note, however, that the search space in Zoph et al. (2017) is vastly larger (10^{28}) than the search space in this work (10^{14}) (see Section 4). Given the results in the previous section indicating $1.8\times$ efficiency gains, we infer that the majority of the $15\times$ speed up is due to the reduced search space. In the future, we plan to run PNAS on the full space (of size 10^{28}), to measure the relative speed, and also the final model quality.

Table 1 also shows a comparison with Liu et al. (2017),

Method	Algo.	Error	Params	Models
NASNet-A ($N = 6, F = 32$) (Zoph et al., 2017)	RL	3.41	3.3M	20,000
NASNet-B ($N = 4$) (Zoph et al., 2017)	RL	3.73	2.6M	20,000
NASNet-C ($N = 4$) (Zoph et al., 2017)	RL	3.59	3.1M	20,000
Hierarchical ($N = 2, F = 128$) (Liu et al., 2017)	EA	3.63 ± 0.10	61.3M	7000
Hierarchical ($N = 2, F = 64$) (Liu et al., 2017)	EA	3.75 ± 0.12	15.7M	7000
Hierarchical ($N = 2, F = 64$) (Liu et al., 2017)	Random	3.91 ± 0.15	14.1M	7000
Hierarchical ($N = 2, F = 64$) (Liu et al., 2017)	Random	4.04 ± 0.2	14.1M	200
PNASNet-5 ($N = 3, F = 48$)	SMBO	3.41 ± 0.09	3.2M	1280
PNASNet-4 ($N = 4, F = 44$)	SMBO	3.50 ± 0.10	3.0M	1024
PNASNet-3 ($N = 6, F = 32$)	SMBO	3.70 ± 0.12	1.8M	768
PNASNet-2 ($N = 6, F = 32$)	SMBO	3.73 ± 0.09	1.7M	512
PNASNet-1 ($N = 6, F = 44$)	SMBO	4.01 ± 0.11	1.6M	256

Table 1. Results on CIFAR-10 of some recent structure learning methods; methods in the bottom block are from this paper. “Algo” is the type of search algorithm that is used (RL = reinforcement learning, EA = evolutionary algorithm, SMBO = sequential model based optimization). “Error” is the top-1 misclassification rate of the best model. “Params” is the corresponding number of parameters. “Models” is the number of models that are trained and evaluated in order to find the best model. Our error rates have the form $\mu \pm \sigma$, where μ is the average validation performance over 15 random trials of fitting and evaluating each model, and σ is the standard deviation.

which uses evolutionary algorithms applied to a similar (but not identical) space of cell structures. Our best model is more accurate than their best (we achieve 3.41% error rate, they achieve 3.63%), and uses significantly fewer parameters (3.2M vs 61.3M), but more importantly, we are also much more efficient: we achieve our best result using just 1280 model evaluations, whereas they need to perform 7000 model evaluations, which is $5 \times$ more.

5.4. Performance of Smaller Models

We also evaluated the performance of the best smaller models that we discover during the search process, which we denote by PNASNet- $\{1, 2, 3, 4\}$. We train each of them using the same hyperparameters as PNASNet-5, other than N and F . We then evaluate the test set performance of each model. We repeat this process 15 times, using different random seeds for the initialization of the parameters. Figure 4 shows the resulting performance for each of the PNASNet- $\{1, 2, 3, 4, 5\}$ models. We can see that the test set error rate decreases as we progress from $b = 1$ to $b = 5$ and eventually at $b = 5$ achieves very similar performance to NASNet-A.

We show these best learned cell structures for $b = 1 : 5$ in Figure 5 and Figure 6. The architectures of PNASNet and NASNet have both similarities and differences. PNASNets and NASNets are wide rather than deep, and they both find connections from H_B^{c-2} (i.e., the previous previous cell) useful. One notable difference is that PNASNet-5 has a maximum block depth of 2, whereas NASNet-A’s Normal cell is entirely flat.

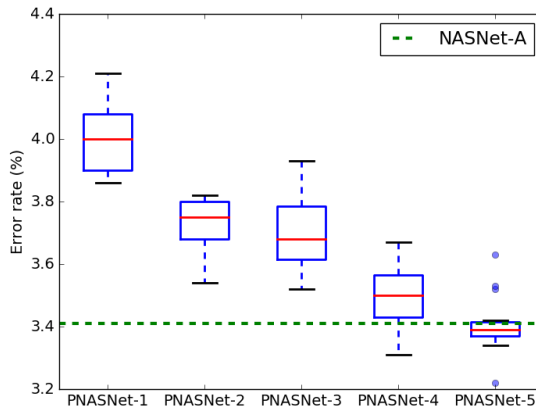


Figure 4. Boxplot of the test performance on CIFAR-10 of the best model with $b \in \{1, 2, 3, 4, 5\}$ blocks found by PNAS. We train and test each model 15 times for 600 epochs; so the spread in quality (vertical axis) is due to randomness in parameter initialization, the SGD optimization process, etc. The horizontal line is the performance of the best model found by the NAS-RL-cell method, which also fits a cell with 5 blocks.

5.5. Effectiveness of the Pruning Process

The predictive accuracy of our surrogate function improves as we collect more training data: the mean predictive error drops from 0.97% when $b = 2$ to 0.48% when $b = 5$. Note that since the child networks are only trained for 20 epochs on CIFAR-10, the validation accuracy across models has a non-negligible variance, making this a noisy training signal. (Indeed, in Liu et al. (2017), they train and evaluate

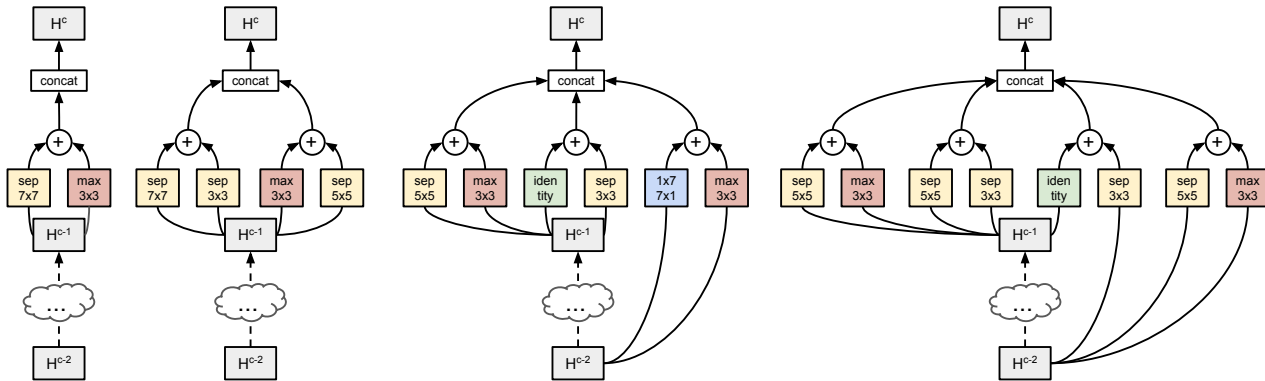


Figure 5. Cell structures used in PNASNet-{1, 2, 3, 4}.

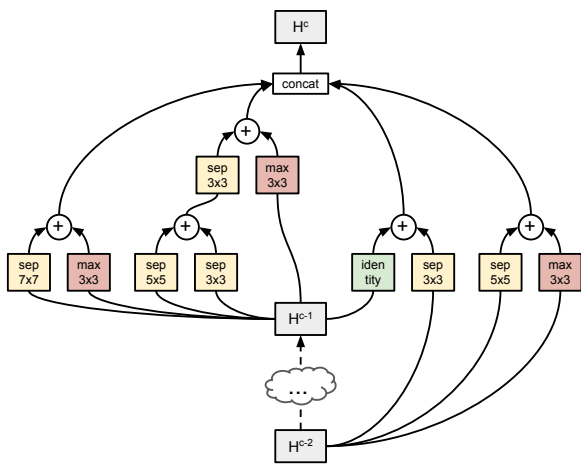


Figure 6. Cell structure used in PNASNet-5.

each candidate model 4 times to reduce the variance.) Furthermore, we get very few of these noisy samples to train on (a total of K data points per iteration). Nevertheless, the predictor seems to provide a useful “steering” signal to the search process.

To measure the effectiveness of the model search process as we move from $b = 1$ to $b = 5$, we compute three metrics: highest validation accuracy, mean validation accuracy, and number of models with > 0.9 validation accuracy among the K child networks. We compare against the random baseline, which randomly selects K models from the entire space $\mathcal{B}_{1:b}$ at each level.

We can see from Figure 7 that regardless of the metric, our PNAS algorithm shows significant gains over the random baseline. In particular, the PNAS models have much higher performance at each step of the search, both in terms of the max and mean performance. In addition, the fraction of high performing models is significantly greater; this can be useful for when we want to find an ensemble of good

models.

5.6. Results on ImageNet Image Classification

Following Zoph et al. (2017), we further demonstrate the usefulness of our learned cell by applying it to ImageNet classification. We conduct experiments under two settings:

- *Mobile*: Here we restrain the representation power of the CNN. Input image size is 224x224, and we limit the number of multiply-add operations to be under 600M.
- *Large*: Here we compare PNASNet-5 against the state-of-the-art models on ImageNet. Input image size is 331x331.

In both experiments we use RMSProp optimizer, label smoothing with value 0.1, auxiliary classifier located at 2/3 of the maximum depth weighted by 0.4, weight decay 4e-5, and dropout of 0.5 in the final softmax layer. In the *Mobile* setting, we use distributed synchronous SGD with 50 workers each with a P100 GPU. On each worker, batch size is 32, initial learning rate is 0.04, and is decayed every 2.2 epochs with rate 0.97. In the *Large* setting, we use 100 P100 workers. On each worker, batch size is 16, initial learning rate is 0.015, and is decayed every 2.8 epochs with rate 0.97. During training, we drop each path with probability 0.3.

The results of the *Mobile* setting are summarized in Table 2. Our PNASNet-5 achieves slightly better performance than NASNet-A (74.2% top 1 accuracy for PNAS vs 74.0% for NASNet-A). Both methods significantly surpass the previous state-of-the-art, which includes the manually designed MobileNet (Howard et al., 2017) (70.6%) and ShuffleNet (Zhang et al., 2017) (70.9%). Table 3 shows that under the *Large* setting, PNASNet-5 achieves comparable performance (82.9% top 1; 96.1% top 5) with previous state-of-

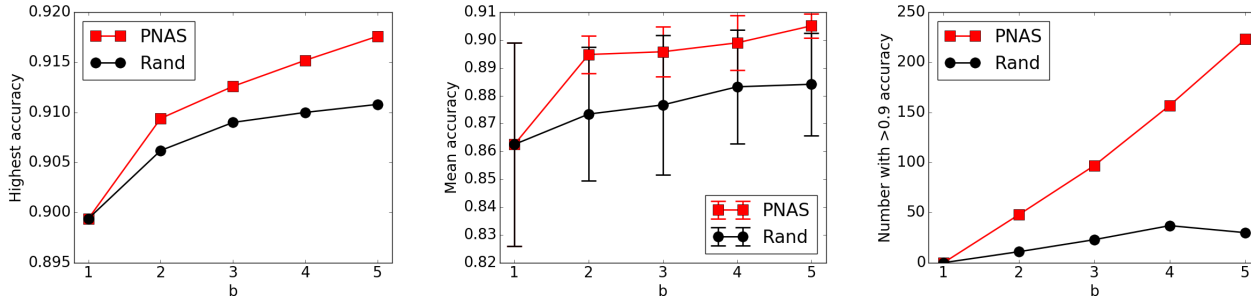


Figure 7. Measuring the effectiveness of the pruning process. We plot three metrics: (a) highest accuracy, (b) mean accuracy (with error bars), and (c) the number of models with > 0.9 accuracy within the $K = 256$ models at each level b . “PNAS” is our algorithm. “Rand” means randomly selecting K models from $\mathcal{B}_{1:b}$.

Model	Params	Mult-Adds	Top 1 (%)	Top 5 (%)
MobileNet-224 (Howard et al., 2017)	4.2M	569M	70.6	89.5
ShuffleNet (2x) (Zhang et al., 2017)	5M	524M	70.9	89.8
NASNet-A ($N = 4, F = 44$) (Zoph et al., 2017)	5.3M	564M	74.0	91.6
PNASNet-5 ($N = 3, F = 54$)	5.1M	588M	74.2	91.9

Table 2. ImageNet classification results in the *Mobile* setting.

Model	Image Size	Params	Mult-Adds	Top 1 (%)	Top 5 (%)
ResNeXt-101 (64x4d) (Xie et al., 2017)	320x320	83.6M	31.5B	80.9	95.6
PolyNet (Zhang et al., 2016)	331x331	92M	34.7B	81.3	95.8
Dual-Path-Net-131 (Chen et al., 2017)	320x320	79.5M	32.0B	81.5	95.8
Squeeze-Excite-Net (Hu et al., 2017)	320x320	145.8M	42.3B	82.7	96.2
NASNet-A ($N = 6, F = 168$) (Zoph et al., 2017)	331x331	88.9M	23.8B	82.7	96.2
PNASNet-5 ($N = 4, F = 216$)	331x331	86.1M	25.0B	82.9	96.1

Table 3. ImageNet classification results in the *Large* setting.

the-art approaches, including SENet (Hu et al., 2017) and NASNet-A.

6. Discussion and Future Work

The main contribution of this work is to show how we can accelerate the search for good CNN structures by using progressive search through the space of increasingly complex graphs, combined with a learned prediction function to efficiently identify the most promising models to explore. The resulting architectures achieve the same level of performance as previous work but with a fraction of the computational cost. In the future, we hope to further improve the efficiency of the search (e.g., by using model-based early stopping), and to scale up the technique so it can be applied to more complex graph structures, such as those used to perform object detection.

Acknowledgements

We thank Quoc Le for inspiration, discussion and support; George Dahl for many fruitful discussions; Gabriel Bender, Vijay Vasudevan for the development of much of the critical infrastructure and the larger Google Brain team for the support and discussions. The first author thanks Lingxi Xie for support.

References

Baker, Bowen, Gupta, Otkrist, Naik, Nikhil, and Raskar, Ramesh. Designing neural network architectures using reinforcement learning. In *ICLR*, 2017a.

Baker, Bowen, Gupta, Otkrist, Raskar, Ramesh, and Naik, Nikhil. Accelerating neural architecture search using performance prediction. *CoRR*, abs/1705.10823, 2017b.

- Brock, Andrew, Lim, Theodore, Ritchie, James M., and Weston, Nick. SMASH: one-shot model architecture search through hypernetworks. *CoRR*, abs/1708.05344, 2017.
- Cai, Han, Chen, Tianyao, Zhang, Weinan, Yu, Yong, and Wang, Jun. Reinforcement learning for architecture search by network transformation. *CoRR*, abs/1707.04873, 2017.
- Chen, Yunpeng, Li, Jianan, Xiao, Huaxin, Jin, Xiaojie, Yan, Shuicheng, and Feng, Jiashi. Dual path networks. *CoRR*, abs/1707.01629, 2017.
- Cortes, Corinna, Gonzalvo, Xavier, Kuznetsov, Vitaly, Mohri, Mehryar, and Yang, Scott. Adanet: Adaptive structural learning of artificial neural networks. In *ICML*, 2017.
- Deng, Jia, Dong, Wei, Socher, Richard, Li, Li-Jia, Li, Kai, and Fei-Fei, Li. Imagenet: A large-scale hierarchical image database. In *CVPR*, 2009.
- Grosse, Roger B, Salakhutdinov, Ruslan, Freeman, William T, and Tenenbaum, Joshua B. Exploiting compositionality to explore a large space of model structures. In *UAI*, 2012.
- He, Kaiming, Zhang, Xiangyu, Ren, Shaoqing, and Sun, Jian. Deep residual learning for image recognition. In *CVPR*, 2016.
- Howard, Andrew G., Zhu, Menglong, Chen, Bo, Kalenichenko, Dmitry, Wang, Weijun, Weyand, Tobias, Andreetto, Marco, and Adam, Hartwig. Mobilenets: Efficient convolutional neural networks for mobile vision applications. *CoRR*, abs/1704.04861, 2017.
- Hu, Jie, Shen, Li, and Sun, Gang. Squeeze-and-excitation networks. *CoRR*, abs/1709.01507, 2017.
- Huang, Furong, Ash, Jordan T., Langford, John, and Schapire, Robert E. Learning deep resnet blocks sequentially using boosting theory. *CoRR*, abs/1706.04964, 2017a.
- Huang, Gao, Liu, Zhuang, Weinberger, Kilian Q., and van der Maaten, Laurens. Densely connected convolutional networks. In *CVPR*, 2017b.
- Hutter, Frank, Hoos, Holger H, and Leyton-Brown, Kevin. Sequential Model-Based optimization for general algorithm configuration. In *Intl. Conf. on Learning and Intelligent Optimization*, Lecture Notes in Computer Science, pp. 507–523, 2011.
- Kingma, Diederik P. and Ba, Jimmy. Adam: A method for stochastic optimization. In *ICLR*, 2015.
- Krizhevsky, Alex and Hinton, Geoffrey. Learning multiple layers of features from tiny images. *Technical report, University of Toronto*, 2009.
- Krizhevsky, Alex, Sutskever, Ilya, and Hinton, Geoffrey E. Imagenet classification with deep convolutional neural networks. In *NIPS*, 2012.
- Lin, Tsung-Yi, Maire, Michael, Belongie, Serge J., Hays, James, Perona, Pietro, Ramanan, Deva, Dollár, Piotr, and Zitnick, C. Lawrence. Microsoft COCO: common objects in context. In *ECCV*, 2014.
- Liu, Hanxiao, Simonyan, Karen, Vinyals, Oriol, Fernando, Chrisantha, and Kavukcuoglu, Koray. Hierarchical representations for efficient architecture search. *CoRR*, abs/1711.00436, 2017.
- Loshchilov, Ilya and Hutter, Frank. SGDR: stochastic gradient descent with restarts. In *ICLR*, 2017.
- Mendoza, Hector, Klein, Aaron, Feurer, Matthias, Springenberg, Jost Tobias, and Hutter, Frank. Towards Automatically-Tuned neural networks. In *ICML Workshop on AutoML*, pp. 58–65, December 2016.
- Miikkulainen, Risto, Liang, Jason Zhi, Meyerson, Elliot, Rawal, Aditya, Fink, Dan, Francon, Olivier, Raju, Bala, Shahrzad, Hormoz, Navruzian, Arshak, Duffy, Nigel, and Hodjat, Babak. Evolving deep neural networks. *CoRR*, abs/1703.00548, 2017.
- Negrinho, Renato and Gordon, Geoffrey J. Deeparchitect: Automatically designing and training deep architectures. *CoRR*, abs/1704.08792, 2017.
- Real, Esteban, Moore, Sherry, Selle, Andrew, Saxena, Saurabh, Suematsu, Yutaka Leon, Tan, Jie, Le, Quoc V., and Kurakin, Alexey. Large-scale evolution of image classifiers. In *ICML*, 2017.
- Schulman, John, Wolski, Filip, Dhariwal, Prafulla, Radford, Alec, and Klimov, Oleg. Proximal policy optimization algorithms. *CoRR*, abs/1707.06347, 2017.
- Shahriari, B, Swersky, K, Wang, Ziyu, Adams, R P, and de Freitas, N. Taking the human out of the loop: A review of bayesian optimization. *Proc. IEEE*, 104(1):148–175, January 2016.
- Simonyan, Karen and Zisserman, Andrew. Very deep convolutional networks for large-scale image recognition. In *ICLR*, 2015.
- Snoek, Jasper, Larochelle, Hugo, and Adams, Ryan P. Practical bayesian optimization of machine learning algorithms. In *NIPS*, 2012.

- Stanley, Kenneth O. Neuroevolution: A different kind of deep learning, July 2017.
- Stanley, Kenneth O and Miikkulainen, Risto. Evolving neural networks through augmenting topologies. *Evol. Comput.*, 10(2):99–127, 2002.
- Szegedy, Christian, Liu, Wei, Jia, Yangqing, Sermanet, Pierre, Reed, Scott E., Anguelov, Dragomir, Erhan, Dumitru, Vanhoucke, Vincent, and Rabinovich, Andrew. Going deeper with convolutions. In *CVPR*, 2015.
- Szegedy, Christian, Vanhoucke, Vincent, Ioffe, Sergey, Shlens, Jonathon, and Wojna, Zbigniew. Rethinking the inception architecture for computer vision. In *CVPR*, 2016.
- Williams, R. Simple statistical gradient-following algorithms for connectionist reinforcement learning. *Machine Learning*, 8:229–256, 1992.
- Xie, Lingxi and Yuille, Alan L. Genetic CNN. In *ICCV*, 2017.
- Xie, Saining, Girshick, Ross B., Dollár, Piotr, Tu, Zhuowen, and He, Kaiming. Aggregated residual transformations for deep neural networks. In *CVPR*, 2017.
- Zhang, Xiangyu, Zhou, Xinyu, Lin, Mengxiao, and Sun, Jian. Shufflenet: An extremely efficient convolutional neural network for mobile devices. *CoRR*, abs/1707.01083, 2017.
- Zhang, Xingcheng, Li, Zhizhong, Loy, Chen Change, and Lin, Dahua. Polynet: A pursuit of structural diversity in very deep networks. *CoRR*, abs/1611.05725, 2016.
- Zhong, Zhao, Yan, Junjie, and Liu, Cheng-Lin. Practical network blocks design with Q-Learning. In *AAAI*, 2018.
- Zoph, Barret and Le, Quoc V. Neural architecture search with reinforcement learning. In *ICLR*, 2017.
- Zoph, Barret, Vasudevan, Vijay, Shlens, Jonathon, and Le, Quoc V. Learning transferable architectures for scalable image recognition. *CoRR*, abs/1707.07012, 2017.